Author(s): Abe, Shinya; Narra, Nathaniel; Nikander, Riku; Hyttinen, Jari; Kouhia, Reijo; Sievänen, Harri

Title: Exercise loading history and femoral neck strength in a sideways fall: A three-dimensional finite element modeling study

Year: 2016

Version:

Please cite the original version:

Abe, S., Narra, N., Nikander, R., Hyttinen, J., Kouhia, R., & Sievänen, H. (2016). Exercise loading history and femoral neck strength in a sideways fall: A three-dimensional finite element modeling study. Bone, 92, 9-17. https://doi.org/10.1016/j.bone.2016.07.021

Exercise loading history and femoral neck strength in a sideways fall: A three-dimensional finite element modeling study

Shinya Abe MSc, Nathaniel Narra MSc, Riku Nikander PhD, Professor, Jari Hyttinen PhD, Professor, Reijo Kouhia PhD, Professor, Harri Sievänen ScD, Research Director

PII: S8756-3282(16)30209-5
DOI: doi: 10.1016/j.bone.2016.07.021
Reference: BON 11090

To appear in: *Bone*

Received date: 7 February 2016
Revised date: 27 July 2016
Accepted date: 27 July 2016

Please cite this article as: Abe Shinya, Narra Nathaniel, Nikander Riku, Hyttinen Jari, Kouhia Reijo, Sievänen Harri, Exercise loading history and femoral neck strength in a sideways fall: A three-dimensional finite element modeling study, *Bone* (2016), doi: 10.1016/j.bone.2016.07.021

Title

Exercise loading history and femoral neck strength in a sideways fall: A three-dimensional finite element modeling study

Names of the authors in order

Shinya Abe[1], Nathaniel Narra[2], Riku Nikander[3,4,5], Jari Hyttinen[2], Reijo Kouhia[1], Harri Sievänen[6]

Shinya Abe, MSc:

[1]Department of Mechanical Engineering and Industrial Systems, Tampere University of Technology, PO Box 589, FI-33101, Tampere, Finland. e-mail: shinya.abe@tut.fi

Nathaniel Narra, MSc:

[2]Department of Electronics and Communications Engineering, BioMediTech, Tampere University of Technology, PO Box 692, FI-33101, Tampere, Finland.

e-mail: nathaniel.narragirish@tut.fi

Riku Nikander, PhD, Professor:

[3]Gerontology Research Center, Department of Health Sciences, University of Jyväskylä, PO Box 35, FI-40014, University of Jyväskylä, Jyväskylä, Finland.

[4]Central Hospital of Central Finland, Keskussairaalantie 19, FI-40620, Jyväskylä, Finland.

[5]GeroCenter Foundation for Aging Research and Development, Viveca, 2nd floor, Rautpohjankatu 8, FI-40700, Jyväskylä, Finland. e-mail: riku.p.nikander@jyu.fi

Jari Hyttinen, PhD, Professor:

[2]Department of Electronics and Communications Engineering, BioMediTech, Tampere University of Technology, PO Box 692, FI-33101, Tampere, Finland.

e-mail: jari.hyttinen@tut.fi

Reijo Kouhia, PhD, Professor:

[1]Department of Mechanical Engineering and Industrial Systems, Tampere University of Technology, PO Box 589, FI-33101, Tampere, Finland. e-mail address: reijo.kouhia@tut.fi

Harri Sievänen, ScD, Research Director:

[6]The UKK Institute for Health Promotion Research, PO Box 30, FI-33501, Tampere, Finland. email: harri.sievanen@uta.fi

No supplemental data is included in this submission.

Corresponding author:

Shinya Abe

MSc, Doctoral Student at the Department of Mechanical Engineering and Industrial Systems,

Tampere University of Technology

Postal Address: PO Box 589, FI-33101, Tampere, Finland.

Street Address: Korkeakoulunkatu 6, FI-33720, Tampere, Finland.

Phone number: +358(0)408400364

email address: shinya.abe@tut.fi

Abstract

Over 90% of hip fractures are caused by falls. Due to a fall-induced impact on the greater trochanter, the posterior part of the thin superolateral cortex of the femoral neck is known to experience the highest stress, making it a fracture-prone region. Cortical geometry of the proximal femur, in turn, reflects a mechanically appropriate form with respect to habitual exercise loading. In this finite element (FE) modeling study, we investigated whether specific exercise loading history is associated with femoral neck structural strength and estimated fall-induced stresses along the femoral neck. One hundred and eleven three-dimensional (3D) proximal femur FE models for a sideways falling situation were constructed from magnetic resonance (MR) images of 91 female athletes (aged 24.7 ± 6.1 years, > 8 years competitive career) and 20 non-competitive habitually active women (aged 23.7 ± 3.8 years) that served as a control group. The athletes were divided into five distinct groups based on the typical loading pattern of their sports: high-impact (H-I: triple-jumpers and high-jumpers), odd-impact (O-I: soccer and squash players), high-magnitude (H-M: power-lifters), repetitive-impact (R-I: endurance runners), and repetitive non-impact (R-NI: swimmers). The von Mises stresses obtained from the FE models were used to estimate mean fall-induced stresses in eight anatomical octants of the cortical bone cross-sections at the proximal, middle, and distal sites along the femoral neck axis. Significantly ($p < 0.05$) lower stresses compared to the control group were observed: the H-I group — in the superoposterior (10%) and posterior (19%) octants at the middle site, and in the superoposterior (13%) and posterior (22%) octants at the distal site; the O-I group — in the superior (16%), superoposterior (16%), and posterior (12%) octants at the middle site, and in the superoposterior (14%) octant at the distal site; the H-M group — in the superior (13%) and superoposterior (15%) octants at the middle site, and a trend ($p = 0.07$, 9%) in the superoposterior octant at the distal site; the R-I group — in the superior (14%), superoposterior (23%) and posterior (22%) octants at the middle site, and in the superoposterior (19%) and posterior (20%) octants at the distal site. The R-NI group did not differ significantly from the control group. These results suggest that exercise loading history comprising various impacts in particular is associated with a stronger femoral neck in a falling situation and may have potential to reduce hip fragility.

Keywords. Bone strength; Finite element modeling; Exercise; Falling; Osteoporosis; Hip Fracture

1. Introduction

Bone structure adapts to habitual mechanical loading [1,2]. Walking, as the predominant form of human locomotion, causes higher compressive stress at the inferior cortex and smaller tensile stress at the superior cortex of the femoral neck. This asymmetric loading results in a thicker inferior and thinner superior cortical bone [3,4]. With ageing, cortical thinning becomes evident; the thickness of the posterior part of the superolateral cortex, called the superoposterior cortex, declines from a mean 1.6 mm at the age of 25 to 0.3 mm at the age of 85 years in females [4,5]. Mayhew and colleagues [4] suggested that the thinning of the superoposterior cortex contributes significantly to hip fragility. Cortical thinning increases the elastic instability of the cortical shell and can lead to a fracture because of local buckling under compressive load [4]. When one falls sideways, the superolateral cortex experiences unusually high compressive stress due to a high impact force imposed on the greater trochanter [6,7]. The peak magnitude of such a fall-induced stress can be 4 times greater than the stress induced by normal gait [3]. Accordingly, it has been speculated that the fracture initiates from this thin cortical layer of the superolateral region [4,7,8]. Several finite element (FE) modeling and cadaveric experimental studies have consistently shown that a sideways fall exposes the femoral neck to the greatest risk of a fracture [7,9–13]. Indeed, over 90% of hip fractures are directly caused by falls [14,15]. Therefore, if the superolateral cortical thickness could be maintained or even increased with appropriate exercise training, bone strength may be maintained and hip fracture risk reduced in old age.

In our previous studies [16,17], we found that female athletes with a history of high impact and/or impact exercises from unusual directions have higher areal bone mineral density (aBMD), section modulus, and thicker cortical bone of the femoral neck including the superolateral cortex. However, the influence of this exercise-induced structural benefit on femoral neck strength in the sideways fall was not examined. Several FE modeling studies have been conducted to obtain a better understanding of the hip fracture mechanism [3,6,9,11–13,18–22]. To the best of our knowledge, however, no FE modeling study has so far been conducted to investigate the influence of specific exercise loading

history on the structural strength of the femoral neck in a falling situation. In particular, it is not known whether specific exercise loading history is associated with lower stresses during a fall.

The purpose of the present study is to investigate whether the femoral necks adapted to distinct exercise loading patterns show different stress profiles in a sideways fall. For this purpose, proximal femur FE models were created from three-dimensional (3D) image data of 111 female participants with distinct exercise loading histories. These results are expected to provide further insight into the potential of specific exercise types in strengthening the proximal femur and alleviating hip fracture risk.

2. Materials and Methods

2.1. Participants

Magnetic resonance (MR) image data of proximal femurs from 91 adult female athletes (aged 24.7 ± 6.1 years) competing actively at national or international level and 20 habitually active, but non-competitive female control participants (aged 23.7 ± 3.8 years) were obtained from our previous study [17]. The study protocol was approved by the Ethics Committee of the Pirkanmaa Hospital District, and written informed consent was obtained from each participant before the study.

The athletes were recruited from national sports associations and local athletic clubs, and the control participants were mostly students from local medical and nursing schools. The control participants did recreational exercise 2–3 times a week, but had previously never taken part in any competitive sports. The athletes comprised nine triple-jumpers, ten high-jumpers, nine soccer players, ten squash players, 17 power-lifters, 18 endurance runners, and 18 swimmers. According to our previous exercise classification scheme [16,23], the athletes were divided into five different groups based on the typical loading patterns of their sports: high-impact (H-I) (triple- and high-jumpers); odd-impact (O-I) (soccer and squash players); high-magnitude (H-M) (power-lifters); repetitive-impact (R-I) (endurance runners); and the repetitive, non-impact group (R-NI) (swimmers).

Wearing only light indoor clothing without shoes, the body height and weight of the participants were measured using standard methods. Questionnaires were completed by all participants in order to obtain their training history including weekly sport-specific training hours and the number of training sessions during at least the five preceding years. Other information such as medications, diseases, menstrual status, use of hormonal contraceptives, calcium intake, alcohol, smoking, coffee consumption, and previous injuries and fractures was also collected [17].

2.2. MR image scanning procedure

The hip regions of all participants were scanned using a 1.5-T MR imaging system (Avanto Syngo MR B15, Siemens, Erlangen, Germany). The scanned region covered the proximal femur from the top of the femoral head to the subtrochanteric level of the femoral diaphysis. Using two half-Fourier acquisition single-shot turbo spin-echo localization series, sagittal, axial, and coronal images of the hip region of the dominant side were scanned. The reconstructed imaging plane was adjusted so that the cross-sectional plane of the femoral neck was perpendicular to the femoral neck axis. The MR imaging sequence used was a standardized axial T1-weighted gradient echo volumetric interpolated breath-hold (VIBE)-examination with the following parameters: FOV 35×26 cm, TR 15.3 ms, TE 3.32 ms, slice thickness 1 mm without gaps, echo train length = 1, flip angle =10°, matrix 384×288, the in-plane resolution (pixel size) 0.9 mm×0.9 mm [17].

2.3. FE model construction

The MR images of all participants were first manually segmented by delineating the periosteal and endocortical boundaries of the cortical bone using a touch panel (Wacom Tablet Cintiq 12WX, Wacom Technology Corp., Vancouver, WA, USA) with ITK-SNAP (www.itksnap.org) image processing software [24]. The in vivo precision of periosteal and endocortical delineations of the femoral neck cortex is about 1% [17,25]. The segmented bone geometries were then converted into a volume mesh using the free mesh generation MATLAB (MathWorks, Inc., Natick, MA, USA) tool called iso2mesh [26]. The surface was then smoothed in MeshLab (Visual Computing Lab – ISTI – CNR, http://meshlab.sourceforge.net/) using a method described by Taubin [27]. This method was

chosen for its known performance in minimizing the shrinkage of the geometry during the smoothing process. The smoothed proximal femur geometries were subsequently imported into SolidWorks (SolidWorks Corp., Waltham, MA, USA) for the generation of 3D solid bodies. The resulting proximal femur geometry comprised individually segmented cortical bone and trabecular bone volumes, the latter denoting the volume within the endocortical bone boundary. Although trabecular bone is truly a porous structure, in the present study it was modeled as a non-porous homogeneous material.

The individual 3D solid body geometries of the proximal femur were finally imported into ANSYS 16.1 (ANSYS Inc., Houston, PA, USA) for the FE meshing and model analysis. The ANSYS Academic Research license was obtained from CSC – IT Center for Science Ltd. (Espoo, Finland). First, the femoral neck geometry was defined (Fig. 1), and then similar boundary conditions (BCs) from the previous studies [22,28] were used in the present study. Force and restraining BCs were applied through the femoral head and trochanter-protecting polymethyl methacrylate (PMMA) caps, and aluminum distal pot (Fig. 2). A 10-noded tetrahedral finite element was used to mesh all materials. The element size was set to 1mm for the entire proximal femur bone geometry, the caps, and the boundary between the distal end of the bone and the distal pot. The body of the distal pot, away from the boundary, was meshed with a 4 mm element size. The maximum error in octant stress (described in Section 2.4) was estimated based on the converged solution that was obtained by extrapolating the results from the 3 mm, 2 mm, 1.5 mm, 1 mm, and 0.75 mm FE mesh models. The estimated errors were 6.7%, 4.2%, 3.4%, 2.4%, and 2.1% for the 3 mm, 2 mm, 1.5 mm, 1 mm, 0.75 mm meshes, respectively. Based on these findings, a 1 mm mesh element size for the models in this study was deemed satisfactory. On average, each bone model comprised approximately 1,600,000 elements and 2,300,000 nodes. The cortical and trabecular bones of the proximal femur were modeled as homogeneous isotropic, linear elastic materials. Young's moduli of 17 GPa [29–31], 1500 MPa [30,31], 70 GPa [22], and 2 GPa [22] were set for the cortical, trabecular bone, the aluminum distal pot, and the protecting PMMA caps, respectively. Poisson's ratio was assumed as 0.33 [29–31] for all materials.

To simulate sideways falling, the most commonly used force direction from previous experimental studies [10,32,33] was chosen. The femoral shaft was tilted at 10° with respect to the ground and the femoral neck was internally rotated by 15° (Fig. 2) [10,32,33]. The individual impact force was estimated using the equation proposed by Bouxsein et al. [34]:

$$F_{peak} = \sqrt{2gh_{cg}KM},$$

where g is the gravitational constant (9.81 m/s^2), h_{cg} is the height of the center of gravity of the body assumed as 0.51×height(m), K is the stiffness constant (71 kN/m), and M is the effective mass calculated by ($\frac{7}{20}$ × total body mass).

The force described above was then applied to the entire upper face of the femoral head cap at a defined angle while the trochanter cap was restrained in the direction of the force (Fig. 2) [22]. The femoral head and trochanter caps covered a depth of 5 mm of the femoral head and the lateral side of the trochanter [6]. The distal pot was placed at 15–20 mm below the most projected part of the lesser trochanter of each proximal femur. The distance between the most proximal part of the proximal femur to the distal part of the aluminum pot was in the range of 280–306 mm and was similar to the previous study [35]. A hinge-type restraining BC was applied to the distal side of the aluminum pot. This allowed nodes at the hinge-axis to freely rotate in the quasi-frontal plane, while all other degrees of freedom were constrained [22,28].

2.4. FE derived stress within the femoral neck cortical bone

From each FE model, the nodal cortical von Mises stresses were calculated for the entire femoral neck region. These von Mises stresses were imported into MATLAB for further post-FE analysis. The entire femoral neck region was first divided into three sub-volumes along the femoral neck axis: proximal, middle, and distal volumes. For clarity, these sub-volumes are henceforth referred to as proximal, middle, and distal sites (Fig. 1). This division was performed so that the length of the most superior surface was equal for each site. Next, these three sites were divided into equal 45° octant regions each representing different anatomic directions of the respective cross-section of the femoral

neck. This octant division was performed similar to previous studies [4,17,36,37] except that the femoral neck axis was used as a reference for the center of the octant instead of the geometric centroid. In the present study, the femoral neck axis was defined similar to a previous study [38] so that it goes through the center of the femoral head and the geometric center of the thinnest femoral neck cross-section. The center of the femoral head was identified as the center of the sphere that best fitted the periosteal surface. The octants were anatomically defined as inferior (I), inferoanterior (IA), anterior (A), superoanterior (SA), superior (S), superoposterior (SP), posterior (P), and inferoposterior region (IP) (Fig. 1). For each individual proximal femur FE model, the mean cortical von Mises stresses in each octant (*octant cortical stress*) were calculated for all three sites.

2.5. Statistical Analysis

Statistical analyses were performed with SPSS 22.0 (IBM Corp., Armonk, NY, USA). Mean and SD were given as descriptive statistics. Differences in octant cortical stresses in the three sites between each exercise group and the control group were estimated by multivariable analysis of covariance (MANCOVA) using the individual impact force as a covariate. Exercise groups were not compared to each other. Sidak correction was used to control for multiple comparisons in the post-hoc tests. Logarithmic transformations of the octant cortical stresses were performed prior to MANCOVA to control skewness of the data. Percentage differences of the octant cortical stress between each exercise loading group and control group were calculated by taking anti-log of the impact force-adjusted mean octant cortical stress. A p value of less than 0.05 was considered statistically significant.

3. Results

3.1. Descriptive data of participants

Table 1 shows the descriptive data of age, sport-specific training hours/week, training sessions/week, duration of competitive career, height, body weight (BW), and estimated impact force in each exercise loading and control group. Further details of body composition and muscular performance have been reported previously [17]. In addition to a competitive career of more than 8 years, athletic participants

clearly had much longer training hours and more training sessions per week compared with the non-competitive habitually active control participants.

3.2. Octant cortical stresses in general

Figure 3 shows the unadjusted mean octant cortical stresses for proximal, middle, and distal femoral neck sites for each group. At the proximal site, higher stress levels were generally observed in the inferior and inferoposterior regions, while at the middle site higher stress levels were generally evident in the superior, superoposterior, and posterior regions. At the distal site, higher stresses were generally observed in the posterior region and became prominent in the superoposterior region. Figure 4 presents example subjects from each group of the study population to illustrate typical stress distributions in each group. Stresses higher than 185 MPa were observed in the region spanning the superoposterior and posterior part of the femoral neck. Notably, a large contiguous area of > 185 MPa stresses can be seen in the stress distributions of the repetitive non-impact group (R-NI) and the control proximal femora. Table 2 shows the impact force-adjusted mean percentage differences in octant cortical stresses for the proximal, middle, and distal femoral neck sites between each exercise loading group and the control group.

3.2.1. Proximal octant stress

The high-impact (H-I) group had significantly lower octant stresses ($p < 0.05$) than in the control group in the inferior (21%), inferoanterior (29%), superoanterior (9%), superoposterior (12%), posterior (15%), and inferoposterior (17%) octants. The odd-impact (O-I) group had significantly lower stresses in the superoposterior (14%) and posterior (12%) octants. The high-magnitude (H-M) group had significantly lower stresses in the superoposterior (16%) and posterior (12%) octants. The repetitive-impact (R-I) group had significantly lower stresses in the inferior (14%), inferoanterior (19%), anterior (16%), superoanterior (13%), superior (12%), superoposterior (21%), posterior (22%), and inferoposterior (15%) octants.

3.2.2. Middle octant stress

The H-I group had significantly lower octant stresses ($p < 0.05$) than in the control group in the inferior (32%), inferoanterior (29%), anterior (16%), superoposterior (10%), posterior (19%), and inferoposterior (25%) octants. The O-I group had significantly lower stresses in the inferior (17%), inferoanterior (17%), anterior (14%), superoanterior (14%), superior (16%), superoposterior (16%), and posterior (12%) octants. The H-M group had significantly lower stresses in the superior (13%) and superoposterior (15%) octants. The R-I group had significantly lower stresses in the inferior (20%), inferoanterior (21%), anterior (18%), superoanterior (13%), superior (14%), superoposterior (23%), posterior (22%), and inferoposterior (17%) octants. Also, a trend for lower stresses when compared to controls was observed in the H-I group in the superoanterior ($p = 0.07$, 11%) octant.

3.2.3. Distal octant stress

The H-I group had significantly lower octant stresses ($p < 0.05$) than in the control group in the inferior (24%), inferoanterior (18%), superoposterior (13%), posterior (22%), and inferoposterior (22%) octants. The O-I group had significantly lower stresses in the inferior (16%), inferoanterior (13%), and superoposterior (14%) octants. The R-I group had significant lower stresses in the inferior (17%), inferoanterior (17%), anterior (18%), superoanterior (18%), superoposterior (19%), posterior (20%), and inferoposterior (16%) octants. Also, trends for lower stresses when compared to controls were observed in the H-I group in the anterior ($p = 0.06$, 15%) and superoanterior ($p = 0.06$, 16%) octants. In the O-I group, trends for lower stresses were observed in the superoanterior ($p = 0.08$, 14%) and posterior ($p = 0.07$, 9%) octants. In the H-M group, similar trends were observed in the superoposterior ($p = 0.07$, 9%) octant and in the superior ($p = 0.08$, 17%) octant in the R-I group.

4. Discussion

In this large FE modeling study of female athletes, the association of specific exercise loading history with femoral neck structural strength in a sideways falling situation was elaborated. As expected from the findings of previous studies [6,7], high stresses were primarily distributed over the superolateral cortex region of the femoral neck: specifically, in the superior, superoposterior, and posterior octants

at the middle site, and in the superoposterior and posterior octants at the distal sites. Present results suggest that exercise loading history during adolescences and early adulthood that involves either high impacts (H-I), impacts from unusual directions (O-I), a large number of repetitive impacts (R-I), or extreme muscle forces (H-M) is associated with significantly lower (10–23%) fall-induced stresses at these vulnerable femoral neck regions (the five octants listed above) when compared to the control group. Importantly, the highest octant stresses were observed in the fracture-prone posterior part of the superolateral cortex region (superoposterior octant in the distal site in Fig.1 and Fig.3), which is in agreement with the findings of a study by Mayhew et al. [4]. We found that the femoral neck in the H-I, the O-I, and the R-I groups experienced significantly lower (13–19%) stress in this octant compared to the control group. Although a significant difference was not observed, the H-M group exhibited a trend for lower stress (p = 0.07, 9%) in the same octant. These results may translate into a reduced risk of hip fractures caused by falling.

The present findings are largely explained by the specific structural adaptation of the cortical bone to impact loading. Previously, Nikander et al. [17] found that the femoral neck of athletes in the H-I group had a thicker cortex in the inferior, anterior, and posterior quadrants, while the O-I group had a consistently thicker cortex in the anterior, posterior, and superior quadrants of the femoral neck. Notably, the lower stresses in the inferior, inferoanterior, and inferoposterior octant regions in the H-I group can be attributed to a very thick inferior cortex: approximately 60% thicker than in the habitually active control group [17].

A particularly interesting finding in the present study was that the femoral neck in the R-I (endurance runners) group also showed significant and similar low stresses to those observed in the H-I group. Previously, Nikander et al. [17] reported that the cortical bone of the femoral neck in the R-I group was not thicker than in the control group. This indicates that the lower stresses in the R-I may be attributed to other geometrical factors, that is, the more circular shape of the femoral neck cross-section shown by Narra et al. [39]. Basically, a more circular bone is mechanically more robust in all directions than an oval shaped bone. Sievänen et al. [40] observed that physically more active

medieval people had a more circular femoral neck cross-section in contrast to present-day people who have a more oval-shaped cross-section. It was estimated that the oval-shaped femoral neck of present-day people may experience 1.3–1.5 times higher fall-induced stress in a sideways fall than the circular femoral neck of the medieval people [40]. This estimation is consistent with the results of the present study that show almost 20% lower stress in the R-I group than in the control group. Running (or walking) is a natural form of locomotion and a common type of exercise. In particular, the human skeleton is particularly fitted for endurance running [41], but as alluring as the present finding is from the evolutionary point of view, the beneficial results in the endurance running group remain at best speculative and warrant further elaboration.

The R-NI group showed no apparent reduction in stress at any femoral neck octant. This agrees with the findings by Nikander et al. [17] that showed no exercise-related benefit to the cortical geometry among swimmers. The typical movements in swimming require a lot of repetitive muscle contractions and can be intensive, but they are also smooth and without impacts. The H-M group, in turn, showed less reduced octant stresses compared to the control group than the H-I, O-I, and R-I groups did in spite of extreme muscle forces involved in power-lifting (e.g., a squat). Again, this is likely attributable to the inherent nature of movement. During H-M exercises, the movement is slow by nature, and therefore its rate of loading is low.

Moderate to high ground reaction forces and a high rate of force development due to the ground impact are common factors in exercise loading that seem to be beneficial for femoral neck strength. Peak vertical ground reaction forces are 12–20 times BW [42,43] for H-I exercise, 2.5–3.5 times BW [44–46] for O-I exercise, 2–3 times BW [47] for H-M exercise (squat), and 2–2.5 times BW [48,49] for R-I exercise while the estimated impact loading rates (BWs^{-1}) are about 400–480 BWs^{-1} [42], 20–180 BWs^{-1} [44,45], 5–6 BWs^{-1} [47], and 60–150 BWs^{-1} [48–50], respectively. In swimming, peak reaction force and loading rate at the push-off phase of turning are estimated to be less than 1.5 times BW [51,52] and less than 10 BWs^{-1} [51], respectively. Such a combination of reaction force and loading rate in the R-NI exercise seems to be insufficient to improve femoral neck strength. While

ground reaction force in the H-M exercise may be similar in magnitude to those in the O-I and R-I exercises, the rate of force development is significantly lower. In light of the results for the H-M group, this indicates that in spite of the moderate-to-high ground reaction force, the stimulus for beneficial geometric adaptation seems to be diminished by the lower rate of loading. Differing from power-lifting (squat, bench press, and deadlift), weightlifting movements such as the snatch, clean, and jerk are explosive and involve more impact: peak vertical ground reaction forces are 2.5–4 times BW and estimated impact loading rates vary from about 10–50 BWs^{-1} [53–56]. This warrants further investigation of femoral neck strength among weightlifters.

The mean starting ages of the competitive careers of the athletic participants were the following: H-I = 12.2 years; O-I = 15.7 years; H-M 19.5 years; R-I = 16.5 years; R-NI =10.6 yrs. Accordingly, the H-M group started their sport-specific career the latest of any groups and their careers were also the shortest (mean 8 years) at the time of the study. The H-I group started their career at the age of 12.2 years, which is 7 years earlier than that of the H-M group. Indeed, the starting age of 19.5 years of the H-M group is almost close to skeletal maturity [57]. It is well established that starting the exercise training in early adolescence is the most beneficial for bone strength compared with a later start of training [58]. Lorentzon et al. [59] reported that higher aBMD, cortical bone size, and trabecular density were observed among those who started their training career before the age of 13 than those who started their training later. Further, the duration of the training in adolescence is associated with improved bone traits as well [59,60]. This being the case, the odds of finding a clear exercise-related reduction in fall-induced stress in the H-M group may have been attenuated. However, it is worth noting that starting intensive power-lifting exercises (squat, bench press, and deadlift) at an early age is not recommended, which may explain the later starting age in the H-M group. On the other hand, it is likely that the H-M group was involved in various, less specific exercise training during adolescence.

Observed reductions in the octant stress (10–30%) along the femoral neck in the sideways falling situation, attributable to exercise-induced structural adaptations, may be clinically important. It is

noteworthy that the control group was comprised of young healthy women who did recreational exercises 2–3 times a week. Thus, our control participants were physically active, but not athletes. This being the case, it is possible that actual exercise-induced benefit in the femoral neck strength in sideways falling could be even higher when compared with the average, less physically active population.

As to the clinical relevance of the present results, caution is needed. Since the data were obtained from young female athletes, the results cannot be extrapolated to the general population. Despite the clear benefits, H-I exercise does not provide a panacea against hip fragility and fractures. Extreme impact forces (12–20 times BW) [42,43] in the H-I exercises are obviously too risky not only for older people but also for sedentary people regardless of age. Since the O-I and R-I exercises produce moderate impacts, the risk of musculoskeletal injuries remains lower. Thus, exercise involving impacts from unusual directions and a large number of repeated impacts may offer a more feasible and equally effective option to increase femoral neck strength. For the young, physically active, and/or fit people, not only O-I and R-I exercises but also appropriate H-I exercises are feasible in order to maintain and/or increase femoral neck strength. It is worth mentioning that along with O-I and R-I exercises (e.g. jogging), H-M exercises (squat, deadlift, etc.) may also be beneficial for the overall health of the proximal femur for people with a sedentary background or the elderly. This is, of course, contingent on the people having no preexisting musculoskeletal maladies, having sufficient mobility, and weights being chosen according to their physical conditioning.

Another important question is whether the exercise-induced skeletal benefits from early adulthood can be sustained into old age. It is known that the exercise-induced bone thickening during growth occurs through new bone formation on the periosteal bone surface, while the age-related bone loss takes place at the endocortical bone surface [2]. Should the femoral neck cortical bone be thicker during young adulthood, it may be more resistant against fractures in old age. It is noteworthy that retired ice hockey and soccer players more than 60 years old have lower fracture risk compared to matched controls despite some loss in exercise-induced high aBMD due to retirement from sports

[61]. This finding indicates that the exercise-induced structural benefits to the femoral neck during young adulthood may be sustained into old age and highlights the importance of exercise in adolescence and young adulthood in terms of preventing future hip fractures. Further, the effect of exercise on bone may vary depending on the period of life. During adolescence, exercise can increase bone strength, and continued exercise may help maintain exercise-induced bone strength in adulthood**.** Moreover, exercise may attenuate a decrease in bone strength due to age-related bone loss [60].

The major strength of the present study is the large total sample size of 111 individual FE models that represent a variety of distinct exercise loading histories. This makes the present study one of the largest proximal femur FE modeling studies. Further, the large total sample size made it possible to divide the athletes into smaller subgroups, which enabled us to investigate the association of the distinct exercise loading pattern with femoral neck strength in a sideways falling situation. However, the marginal differences in the H-M group, despite group-differences of a similar magnitude, indicate limited statistical power in some subgroup analyses.

In addition to somewhat limited statistical power, there are other limitations as well. The main limitation was the use of the MR images for the construction of the proximal femur geometry which was not validated against actual mechanical testing. While QCT would have provided high-resolution image data on femoral neck geometry and bone apparent density, MR imaging has been found to be adequately valid for the assessment of cortical geometry [25,62]. The pixel size in the previous QCT-based proximal femur studies [13,19,20] has been around 0.5 mm in contrast to the 0.9 mm pixel size in the present study. Obviously, a higher in-plane resolution would have provided a more accurate segmentation of the cortical bone. Therefore, to comply with valid QCT-based proximal femur FE modeling studies, we adopted similar BCs and loading conditions [22,28]. In the present study, however, trabecular bone was modeled as a non-porous homogeneous structure in contrast to its actual non-uniform structure [63], which could cause < 10% error in the maximum stress reported in the literature [19]. However, according to Koivumäki et al., inclusion of the trabecular bone in the sideways falling FE models may not play a crucial role, and the proximal femoral strength can be

evaluated with reasonable accuracy using a cortical bone FE model only [64]. Further, Holzer et al. [65] reported that the complete removal of the trabecular bone led to a relatively small reduction in bone strength while the cortical bone is primarily responsible for load bearing and transmitting forces. Indeed, the present study mainly focused on evaluating the influence of cortical geometry on the stress distribution in the simulated sideways fall while modeling the trabecular bone as non-porous homogeneous material in every individual model. While the use of QCT-based FE models would have also allowed the estimation of inhomogeneous elastic properties using the voxel-based Hounsfield unit data (density) [11–13,18–22], the assumption of homogeneous material properties is acceptable. Taddei et al. [19] compared the homogeneous proximal femur bone model with the inhomogeneous model and found only a marginal improvement in accuracy of prediction; R^2 between FE predicted stress and experimental stress was 0.91 for the inhomogeneous model and 0.89 for the homogeneous model. Finally, exposing fertile young adult women to ionizing radiation from QCT for non-diagnostic purposes would have been ethically unacceptable.

5. Conclusion

The present FE study is the first study that employed a large number of individual 3D proximal femur FE models obtained from young adult female athletes representing distinct exercise loading patterns. The results showed that the athletes with a history of impact exercises from endurance running induced repetitive impacts, soccer and squash induced odd direction impact, to extreme vertical jumping sports showed clinically relevant lower stresses at the fracture prone regions of the femoral neck in a sideways falling simulation. In addition to impacts, high magnitude strength training may also be beneficial for maintaining the robustness of the femoral neck. This requires further study, however. The results of this study also give new insights into the prevention of hip fragility with targeted exercises.

Acknowledgements

The authors thank all study participants. We also thank Antti Ylinen, DSc, and Ossi Heinonen, MSc, for assisting in the construction of the FE models and Peter Heath, MA, for the language editing.

Funding

This work was supported by Tampere University of Technology's (TUT) Graduate School; the Doctoral Education Council of Computing and Electrical Engineering of TUT; and Human Spare Parts project funded by the Finnish Funding Agency for Technology and Innovation (TEKES).

Disclosures

All authors state that they have no conflicts of interest.

Authorship

All authors contributed to the study design. NN, RN, JH, and HS were responsible for the data collection. Modeling and simulation were performed by SA and supervised by JH and RK. Data analysis was performed by SA, NN, RN, RK, and HS. The manuscript was drafted by SA and HS. All authors are responsible for revising and approving the final version of manuscript. SA takes responsibility for the integrity of the data analysis.

References

[1] H.M. Frost, Bone's mechanostat: A 2003 update, Anat. Rec. A. Discov. Mol. Cell Evol. Biol. 275 (2003) 1081–1101.

[2] C. Ruff, B. Holt, E. Trinkaus, Who's afraid of the big bad Wolff?: "Wolff's law" and bone functional adaptation, Am. J. Phys. Anthropol. 129 (2006) 484–498.

[3] J.C. Lotz, E.J. Cheal, W.C. Hayes, Stress distributions within the proximal femur during gait and falls: Implications for osteoporotic fracture, Osteoporos. Int. 5 (1995) 252–261.

[4] P.M. Mayhew, C.D. Thomas, J.G. Clement, N. Loveridge, T.J. Beck, W. Bonfield, C.J. Burgoyne, J. Reeve, Relation between age, femoral neck cortical stability, and hip fracture risk, Lancet. 366 (2005) 129–135.

[5] K.E. Poole, P.M. Mayhew, C.M. Rose, J.K. Brown, P.J. Bearcroft, N. Loveridge, J. Reeve, Changing structure of the femoral neck across the adult female lifespan, J. Bone Miner. Res. 25 (2010) 482–491.

[6] E. Verhulp, B. van Rietbergen, R. Huiskes, Load distribution in the healthy and osteoporotic human proximal femur during a fall to the side, Bone. 42 (2008) 30–35.

[7] P.M. de Bakker, S.L. Manske, V. Ebacher, T.R. Oxland, P.A. Cripton, P. Guy, During sideways falls proximal femur fractures initiate in the superolateral cortex: Evidence from high-speed video of simulated fractures, J. Biomech. 42 (2009) 1917–1925.

[8] R.D. Carpenter, G.S. Beaupré, T.F. Lang, E.S. Orwoll, D.R. Carter, New QCT analysis approach shows the importance of fall orientation on femoral neck strength, J. Bone Miner. Res. 20 (2005) 1533–1542.

[9] C.M. Ford, T.M. Keaveny, W.C. Hayes, The effect of impact direction on the structural capacity of the proximal femur during falls, J. Bone Miner. Res. 11 (1996) 377–383.

[10] T.P. Pinilla, K.C. Boardman, M.L. Bouxsein, E.R. Myers, W.C. Hayes, Impact direction from a fall influences the failure load of the proximal femur as much as age-related bone loss, Calcif. Tissue Int. 58 (1996) 231–235.

[11] J.H. Keyak, S.A. Rossi, K.A. Jones, H.B. Skinner, Prediction of femoral fracture load using automated finite element modeling, J. Biomech. 31 (1997) 125–133.

[12] J.H. Keyak, H.B. Skinner, J.A. Fleming, Effect of force direction on femoral fracture load for two types of loading conditions, J. Orthop. Res. 19 (2001) 539–544.

[13] M. Bessho, I. Ohnishi, T. Matsumoto, S. Ohashi, J. Matsuyama, K. Tobita, M. Kaneko, K. Nakamura, Prediction of proximal femur strength using a CT-based nonlinear finite element method: Differences in predicted fracture load and site with changing load and boundary conditions, Bone. 45 (2009) 226–231.

[14] J.A. Grisso, J.L. Kelsey, B.L. Strom, G.Y. Chiu, G. Maislin, L.A. O'Brien, S. Hoffman, F. Kaplan, Risk factors for falls as a cause of hip fracture in women. The Northeast Hip Fracture Study Group, N. Engl. J. Med. 324 (1991) 1326–1331.

[15] J. Parkkari, P. Kannus, M. Palvanen, A. Natri, J. Vainio, H. Aho, I. Vuori, M. Järvinen, Majority of hip fractures occur as a result of a fall and impact on the greater trochanter of the femur: A prospective controlled hip fracture study with 206 consecutive patients, Calcif. Tissue Int. 65 (1999) 183–187.

[16] R. Nikander, H. Sievänen, A. Heinonen, P. Kannus, Femoral neck structure in adult female athletes subjected to different loading modalities, J. Bone Miner. Res. 20 (2005) 520–528.

[17] R. Nikander, P. Kannus, P. Dastidar, M. Hannula, L. Harrison, T. Cervinka, N.G. Narra, R. Aktour, T. Arola, H. Eskola, S. Soimakallio, A. Heinonen, J. Hyttinen, H. Sievänen, Targeted exercises against hip fragility, Osteoporos. Int. 20 (2009) 1321–1328.

[18] J.H. Keyak, S.A. Rossi, K.A. Jones, C.M. Les, H.B. Skinner, Prediction of fracture location in

the proximal femur using finite element models, Med. Eng. Phys. 23 (2001) 657–664.

[19] F. Taddei, L. Cristofolini, S. Martelli, H.S. Gill, M. Viceconti, Subject-specific finite element models of long bones: An in vitro evaluation of the overall accuracy, J. Biomech. 39 (2006) 2457–2467.

[20] M. Bessho, I. Ohnishi, J. Matsuyama, T. Matsumoto, K. Imai, K. Nakamura, Prediction of strength and strain of the proximal femur by a CT-based finite element method, J. Biomech. 40 (2007) 1745–1753.

[21] Z. Yosibash, N. Trabelsi, C. Milgrom, Reliable simulations of the human proximal femur by high-order finite element analysis validated by experimental observations, J. Biomech. 40 (2007) 3688–3699.

[22] E. Schileo, L. Balistreri, L. Grassi, L. Cristofolini, F. Taddei, To what extent can linear finite element models of human femora predict failure under stance and fall loading configurations?, J. Biomech. 47 (2014) 3531–3538.

[23] R. Nikander, H. Sievänen, K. Uusi-Rasi, A. Heinonen, P. Kannus, Loading modalities and bone structures at nonweight-bearing upper extremity and weight-bearing lower extremity: A pQCT study of adult female athletes, Bone. 39 (2006) 886–894.

[24] P.A. Yushkevich, J. Piven, H.C. Hazlett, R.G. Smith, S. Ho, J.C. Gee, G. Gerig, User-guided 3D active contour segmentation of anatomical structures: Significantly improved efficiency and reliability, Neuroimage. 31 (2006) 1116–1128.

[25] H. Sievänen, T. Karstila, P. Apuli, P. Kannus, Magnetic resonance imaging of the femoral neck cortex, Acta Radiol. 48 (2007) 308–314.

[26] Q. Fang, D.A. Boas, Tetrahedral mesh generation from volumetric binary and grayscale images, in: Proc. - 2009 IEEE Int. Symp. Biomed. Imaging From Nano to Macro, ISBI 2009, IEEE, 2009: pp. 1142–1145.

[27] G. Taubin, Curve and surface smoothing without shrinkage, in: Proc. -1999 IEEE Int. Conf. Comput. Vis. 1995: pp. 852–857.

[28] B. Helgason, S.Gilchrist, O. Ariza, J.D. Chak, G. Zheng, R.P. Widmer, S.J. Ferguson, P. Guy, P.A. Cripton, Development of a balanced experimental-computational approach to understanding the mechanics of proximal femur fractures, Med. Eng. Phys. 36 (2014) 793–799.

[29] M. Lengsfeld, J. Kaminsky, B. Merz, R.P. Franke, Sensitivity of femoral strain pattern analyses to resultant and muscle forces at the hip joint, Med. Eng. Phys. 18 (1996) 70–78.

[30] G.N. Duda, M. Heller, J. Albinger, O. Schulz, E. Schneider, L. Claes, Influence of muscle forces on femoral strain distribution, J. Biomech. 31 (1998) 841–846.

[31] K. Polgár, H.S. Gill, M. Viceconti, D.W. Murray, J.J. O'Connor, Strain distribution within the human femur due to physiological and simplified loading: finite element analysis using the muscle standardized femur model, Proc. Inst. Mech. Eng. H. 217 (2003) 173–189.

[32] A.C. Courtney, E.F. Wachtel, E.R. Myers, W.C. Hayes, Effects of loading rate on strength of the proximal femur, Calcif. Tissue Int. 55 (1994) 53–58.

[33] A.C. Courtney, E.F. Wachtel, E.R. Myers, W.C. Hayes, Age-related reductions in the strength of the femur tested in a fall-loading configuration, J. Bone Joint Surg. Am. 77 (1995) 387–395.

[34] M.L. Bouxsein, P. Szulc, F. Munoz, E. Thrall, E. Sornay-Rendu, P.D. Delmas, Contribution of trochanteric soft tissues to fall force estimates, the factor of risk, and prediction of hip fracture risk, J. Bone Miner. Res. 22 (2007) 825–831.

[35] O. Ariza, S. Gilchrist, R.P. Widmer, P. Guy, S.J. Ferguson, P.A. Cripton, B. Helgason, Comparison of explicit finite element and mechanical simulation of the proximal femur during dynamic drop-tower testing, J. Biomech. 48 (2015) 224–232.

[36] S.L. Manske, T. Liu-Ambrose, D.M. Cooper, S. Kontulainen, P. Guy, B.B. Forster, H.A.

McKay, Cortical and trabecular bone in the femoral neck both contribute to proximal femur failure load prediction, Osteoporos. Int. 20 (2009) 445–453.

[37] C.D. Thomas, P.M. Mayhew, J. Power, K.E. Poole, N. Loveridge, J.G. Clement, C.J. Burgoyne, J. Reeve, Femoral neck trabecular bone: loss with ageing and role in preventing fracture, J. Bone Miner. Res. 24 (2009) 1808–1818.

[38] J.D. Wilson, W. Eardley, S. Odak, A. Jennings, To what degree is digital imaging reliable? Validation of femoral neck shaft angle measurement in the era of picture archiving and communication systems, Br. J. Radiol. 84 (2011) 375–379.

[39] N. Narra, R. Nikander, J. Viik, J. Hyttinen, H. Sievänen, Femoral neck cross-sectional geometry and exercise loading, Clin. Physiol. Funct. Imaging. 33 (2013) 258–266.

[40] H. Sievänen, L. Józsa, I. Pap, M. Järvinen, T.A. Järvinen, P. Kannus, T.L. Järvinen, Fragile external phenotype of modern human proximal femur in comparison with medieval bone, J. Bone Miner. Res. 22 (2007) 537–543.

[41] D.M. Bramble, D.E. Lieberman, Endurance running and the evolution of Homo, Nature. 432 (2004) 345–352.

[42] M.R. Ramey, K.R. Williams, Ground Reaction Forces in the Triple Jump, Int. J. Sport. Biomech. 1 (1985) 233–239.

[43] A. Heinonen, H. Sievänen, H. Kyröläinen, J. Perttunen, P. Kannus, Mineral mass, size, and estimated mechanical strength of triple jumpers' lower limb, Bone. 29 (2001) 279–285.

[44] N. Smith, R. Dyson, L. Janaway, Ground reaction force measures when running in soccer boots and soccer training shoes on a natural turf surface, Sport. Eng. 7 (2004) 159–167.

[45] M.K. Dayakidis, K. Boudolos, Ground reaction force data in functional ankle instability during two cutting movements, Clin. Biomech. 21 (2006) 405–411.

[46] K. Ball, Loading and performance of the support leg in kicking, J. Sci. Med. Sport. 16 (2013) 455–459.

[47] P.A. Swinton, R. Lloyd, J.W. Keogh, I. Agouris, A.D. Stewart, A biomechanical comparison of the traditional squat, powerlifting squat, and box squat, J. Strength Cond. Res. 26 (2012) 1805–1816.

[48] C.F. Munro, D.I. Miller, A.J. Fuglevand, Ground reaction forces in running: A reexamination, J. Biomech. 20 (1987) 147–155.

[49] S. Logan, I. Hunter, J.T. Hopkins, J.B. Feland, A.C. Parcell, Ground reaction force differences between running shoes, racing flats, and distance spikes in runners, J. Sport. Sci. Med. 9 (2010) 147–153.

[50] B. Kluitenberg, S.W. Bredeweg, S. Zijlstra, W. Zijlstra, I. Buist, Comparison of vertical ground reaction forces during overground and treadmill running. A validation study, BMC Musculoskelet. Disord. 13 (2012) 235.

[51] A.D. Lyttle, B.A. Blanksby, B.C. Elliott, D.G. Lloyd, Investigating kinetics in the freestyle flip turn push-off, J. Appl. Biomech. 15 (1999) 242–252.

[52] B.A. Blanksby, D.G. Gathercole, R.N. Marshall, Force plate and video analysis of the tumble turn by age-group swimmers., J. Swim. Res. 11 (1996) 40–45.

[53] P. Comfort, M. Allen, P. Graham-Smith, Comparisons of peak ground reaction force and rate of force development during variations of the power clean, J. Strength Cond. Res. 25 (2011) 1235–1239.

[54] P. Comfort, M. Allen, P. Graham-Smith, Kinetic comparisons during variations of the power clean, J Strength Cond Res. 25 (2011) 3269–3273.

[55] W. Baumann, V. Gross, K. Quade, P. Galbierz, A. Schvvirtz, The snatch technique of world class weightlifiers at the 1985 World Championships, Int. J. Sport Biomech. 4 (1988) 68–89.

[56] M.A. Lauder, J.P. Lake, Biomechanical comparison of unilateral and bilateral power snatch lifts, J. Strength Cond. Res. 22 (2008) 653–660.

[57] H. Haapasalo, P. Kannus, H. Sievänen, M. Pasanen, K. Uusi-Rasi, A. Heinonen, P. Oja, I. Vuori, Development of mass, density, and estimated mechanical characteristics of bones in Caucasian females, J. Bone Miner. Res. 11 (1996) 1751–1760.

[58] P. Kannus, H. Haapasalo, M. Sankelo, H. Sievänen, M. Pasanen, A. Heinonen, P. Oja, I. Vuori, Effect of starting age of physical activity on bone mass in the dominant arm of tennis and squash players, Ann. Intern. Med. 123 (1995) 27–31. doi:10.7326/0003-4819-123-1-199507010-00003.

[59] M. Lorentzon, D. Mellström, C. Ohlsson, Association of amount of physical activity with cortical bone size and trabecular volumetric BMD in young adult men: the GOOD study, J. Bone Miner. Res. 20 (2005) 1936–1943.

[60] C.A. Boreham, H.A. McKay, Physical activity in childhood and bone health, Br. J. Sports Med. 45 (2011) 877–879.

[61] A. Nordström, C. Karlsson, F. Nyquist, T. Olsson, P. Nordström, M. Karlsson, Bone loss and fracture risk after reduced physical activity, J. Bone Miner. Res. 20 (2005) 202–207.

[62] B.R. Gomberg, P.K. Saha, F.W. Wehrli, Method for cortical bone structural analysis from magnetic resonance images, Acad. Radiol. 12 (2005) 1320–1332.

[63] A.G. Robling, A.B. Castillo, C.H. Turner, Biomechanical and molecular regulation of bone remodeling, Annu. Rev. Biomed. Eng. 8 (2006) 455–498.

[64] J.E. Koivumäki, J. Thevenot, P. Pulkkinen, V. Kuhn, T.M. Link, F. Eckstein, T. Jämsä, Cortical bone finite element models in the estimation of experimentally measured failure loads in the proximal femur, Bone. 51 (2012) 737–740.

[65] G. Holzer, G. von Skrbensky, L.A. Holzer, W. Pichl, Hip fractures and the contribution of

cortical versus trabecular bone to femoral neck strength, J. Bone Miner. Res. 24 (2009) 468–474.

Figure captions

Fig. 1. Division of the femoral neck volume into anatomical sites and octants for the estimation of octant cortical stresses. (A) Posterior view of proximal femur. Dark grey-colored geometry defines the femoral neck geometry of interest. The proximal cross-sectional plane of the defined neck geometry was located at the femoral head-neck junction dividing the femoral head and the femoral neck. The distal plane was adjusted so that the distal plane met following conditions: its superior side is close to trochanteric fossa-greater trochanter junction, its anterior side is close to intertrochanteric line, and its inferior side is close to the lesser trochanter. This distal plane divides the trochanteric region and the femoral neck. (B) The division of the defined femoral neck regions into proximal, middle, and distal sites. The length of the superior surface was kept same for all sites. (C) The equal 45° anatomical octant division in the cross-section of the femoral neck. The femoral neck axis was used as the center of octant division.

Fig. 2. Loading/falling angles (A & B) and boundary conditions of the FE model. The femoral shaft was tilted at 10° with respect to the ground (A) and the femoral neck was internally rotated by 15° (B). Force was applied to the whole upper face of the head-protecting cap, at a described angle. A 200 mm long aluminum pot was placed at 15–20 mm below the most projected part of the lesser trochanter of each proximal femur. A hinge-type constraining boundary condition was applied to nodes of the distal face of the aluminum pot. This allowed nodes at the hinge-axis to freely rotate in the quasi-frontal plane, while all other degrees of freedom were constrained. Greater trochanter cap's surface nodes were restrained in the direction of the force (C).

Fig. 3. Group unadjusted mean (SD) octant cortical stress at the proximal, middle, and distal sites of the femoral neck (see Fig. 1). Each bar represents each group's unadjusted mean octant stress with SD. According to the MANCOVA, * and § show the statistical significance of $0.01 \leq p < 0.05$ and $p < 0.01$ respectively.

Fig. 4. Examples of typical von Mises stress distribution from each group. A, B, C, D, E, and F show an example stress distribution from the H-I, O-I, H-M, R-I, R-NI, and control groups, respectively.

Figure information for size and color for printed version.

Figure1: 1 column size, greyscale

Figure2: 1 column size, greyscale

Figure3: 2 column size, greyscale

Figure4: 2 column size, color

Tables

Table 1. Group characteristics.

Group	n	Age (yr)	Sport-specific training hours / week	Training sessions / week	Competing career (yr)	Height (cm)	Weight (kg)	Impact force (N)
H-I	19	22.3 (4.1)	11.5 (2.3)	6.7 (1.4)	10.1 (3.4)	174 (6)	60.2 (5.4)	5102.1 (268.3)
O-I	19	25.3 (6.7)	9.3 (2.7)	5.7 (1.4)	9.6(4.8)	165 (8)	60.8 (8.3)	4991.0 (450.5)
H-M	17	27.5 (6.3)	9.1 (2.7)	5.8 (2.0)	8.0 (4.7)	158 (3)	63.3 (13.2)	4974.0 (531.9)
R-I	18	28.9 (5.6)	10.9 (3.4)	8.7 (2.1)	12.4 (6.7)	168 (5)	53.7 (3.4)	4737.8 (198.2)
R-NI	18	19.7 (2.4)	19.9 (4.5)	11.4 (2.0)	9.1 (2.6)	173 (5)	65.1 (5.6)	5284.7 (251.1)
Control	20	23.7 (3.8)	2.8 (0.9)	2.8 (1.0)	–	164 (5)	60.0 (7.4)	4943.5 (363.6)

Mean and (SD)

Table 2. Impact force-adjusted mean percentage differences (95% CI) in octant cortical stresses for proximal, middle, and distal sites between each exercise group and control group.

	Proximal	*Middle*	*Distal*
Inferior (I)			
H-I	**-20.6 (-28.6 to -11.8)**	**-32.2 (-39.1 to -24.6)**	**-23.6 (-31.5 to -15.0)**
O-I	-3.4 (-11.5 to 5.7)	**-16.6 (-24.2 to -8.3)**	**-15.7 (-23.4 to -7.3)**
H-M	9.4 (0.2 to 19.5)	-1.1 (-10.6 to 9.4)	-1.1 (-12.1 to 11.1)
R-I	**-13.5 (-20.8 to -5.5)**	**-20.0 (-27.1 to -12.4)**	**-17.0 (-25.3 to -7.8)**
R-NI	-0.2 (-10.3 to 10.8)	-3.2 (-13.6 to 8.7)	-4.3 (-14.9 to 7.7)
InferoAnterior (IA)			
H-I	**-28.6 (-36.1 to -19.9)**	**-29.4 (-35.1 to -23.0)**	**-18.0 (-24.2 to -11.1)**
O-I	-9.2 (-18.1 to 0.5)	**-17.2 (-24.1 to -9.8)**	**-12.9 (-20.3 to -4.7)**
H-M	-0.9 (-11.5 to 10.8)	-8.8 (-17.3 to 0.6)	-2.7 (-12.1 to 7.9)
R-I	**-18.5 (-29.3 to -6.4)**	**-20.6 (-28.1 to -12.1)**	**-16.8 (-23.9 to -9.0)**
R-NI	-7.5 (-20.7 to 7.8)	-4.3 (-14.2 to 6.8)	-0.9 (-10.4 to 9.8)
Anterior (A)			
H-I	-6.0 (-13.9 to 2.8)	**-16.2 (-23.5 to -8.4)**	-14.7 (-24.2 to -4.0)
O-I	-8.6 (-16.5 to 0.1)	**-14.3 (-21.9 to -5.7)**	-12.5 (-22.2 to -1.5)
H-M	-2.9 (-12.2 to 7.2)	-7.3 (-16.4 to 2.7)	-3.2 (-14.6 to 9.9)
R-I	**-15.5 (-23.5 to -6.6)**	**-18.0 (-26.3 to -8.7)**	**-18.2 (-27.0 to -8.1)**
R-NI	1.2 (-9.4 to 12.9)	1.6 (-9.8 to 14.3)	-0.9 (-14.2 to 14.2)
SuperoAnterior (SA)			
H-I	**-9.0 (-15.0 to -2.8)**	-11.3 (-19.2 to -2.6)	-15.7 (-25.6 to -4.5)
O-I	-6.2 (-13.6 to 1.5)	**-13.5 (-21.6 to -4.7)**	-14.1 (-23.7 to -3.0)
H-M	-1.8 (-8.8 to 5.9)	-6.9 (-15.2 to 2.1)	-2.1 (-14.6 to 12.2)
R-I	**-13.3 (-20.0 to -6.0)**	**-12.7 (-20.2 to -4.7)**	**-17.6 (-27.5 to -6.5)**
R-NI	-0.5 (-7.9 to 7.7)	0.9 (-9.0 to 11.7)	4.2 (-11.7 to 22.9)
Superior (S)			
H-I	-8.2 (-14.5 to -1.2)	-5.8 (-12.9 to 1.8)	-6.2 (-18.6 to 7.8)
O-I	-8.8 (-16.0 to -1.1)	**-15.5 (-23.5 to -6.7)**	-9.6 (-22.1 to 4.6)
H-M	-5.8 (-13.2 to 2.2)	**-12.5 (-20.1 to -4.0)**	-6.9 (-20.2 to 8.7)
R-I	**-12.3 (-19.5 to -4.6)**	**-13.9 (-20.8 to -6.5)**	-17.0 (-28.4 to -3.7)
R-NI	0.5 (-8.0 to 9.5)	0.5 (-7.5 to 9.1)	2.6 (-12.2 to 19.8)
SuperoPosterior (SP)			
H-I	**-11.9 (-17.9 to -5.3)**	**-9.8 (-15.5 to -3.6)**	**-12.9 (-18.6 to -6.9)**
O-I	**-13.5 (-19.6 to -7.1)**	**-16.1 (-22.6 to -8.8)**	**-13.5 (-20.0 to -6.4)**
H-M	**-15.7 (-22.2 to -8.6)**	**-14.5 (-21.5 to -6.9)**	-9.4 (-16.3 to -2.1)
R-I	**-20.7 (-25.5 to -15.5)**	**-22.6 (-27.9 to -16.7)**	**-19.3 (-24.6 to -13.8)**
R-NI	-6.2 (-14.1 to 2.2)	-0.5 (-7.7 to 7.3)	-0.5 (-7.5 to 7.3)
Posterior (P)			
H-I	**-14.7 (-20.9 to -8.1)**	**-19.3 (-25.0 to -13.2)**	**-21.5 (-26.8 to -15.6)**
O-I	**-11.5 (-17.0 to -5.4)**	**-11.7 (-17.8 to -5.3)**	-9.0 (-15.3 to -2.0)
H-M	**-11.7 (-17.4 to -5.5)**	-7.5 (-14.0 to -0.3)	-4.7 (-12.0 to 3.2)
R-I	**-21.8 (-26.8 to -16.6)**	**-21.5 (-27.1 to -15.5)**	**-20.0 (-25.9 to -13.5)**
R-NI	-8.0 (-15.2 to 0.1)	1.4 (-7.5 to 11.0)	3.3 (-5.6 to 12.8)
InferoPosterior (IP)			
H-I	**-16.6 (-24.0 to -8.6)**	**-25.4 (-32.6 to -17.3)**	**-22.2 (-29.9 to -13.4)**
O-I	-6.0 (-12.1 to 0.6)	-8.6 (-15.7 to -1.1)	-0.2 (-10.4 to 10.9)
H-M	1.2 (-5.8 to 8.6)	5.4 (-3.3 to 14.8)	6.7 (-4.7 to 19.5)
R-I	**-15.3 (-21.5 to -8.6)**	**-17.0 (-24.0 to -9.5)**	**-15.9 (-24.7 to -5.8)**
R-NI	-5.8 (-13.7 to 2.7)	0.7 (-9.5 to 12.3)	9.4 (-3.9 to 24.5)

Statistically significant p values ($p < 0.05$) based on MANCOVA are shown in bold.

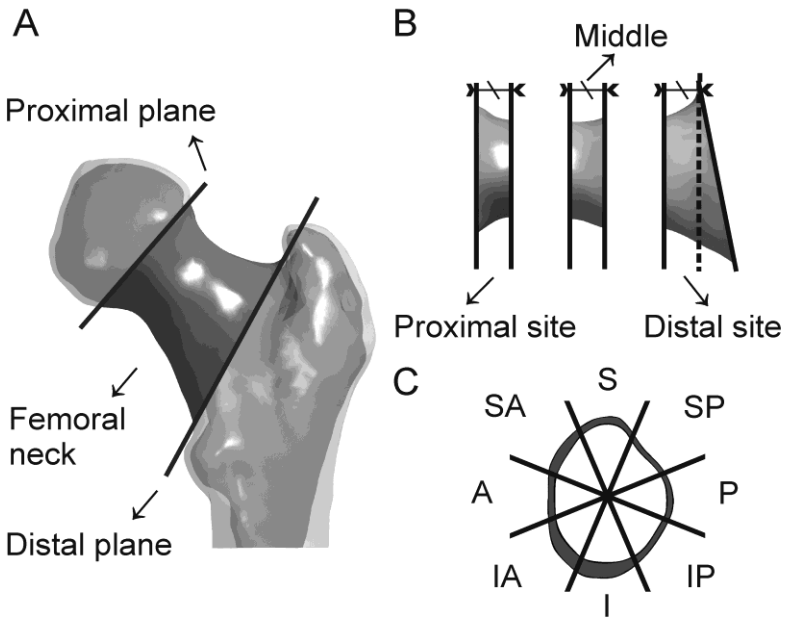

Figure 1

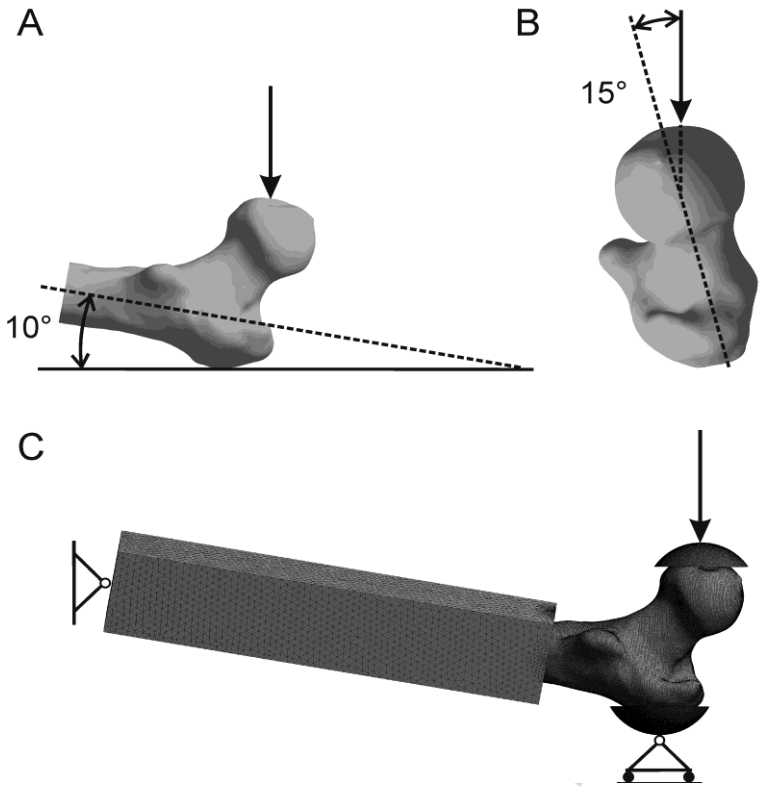

Figure 2

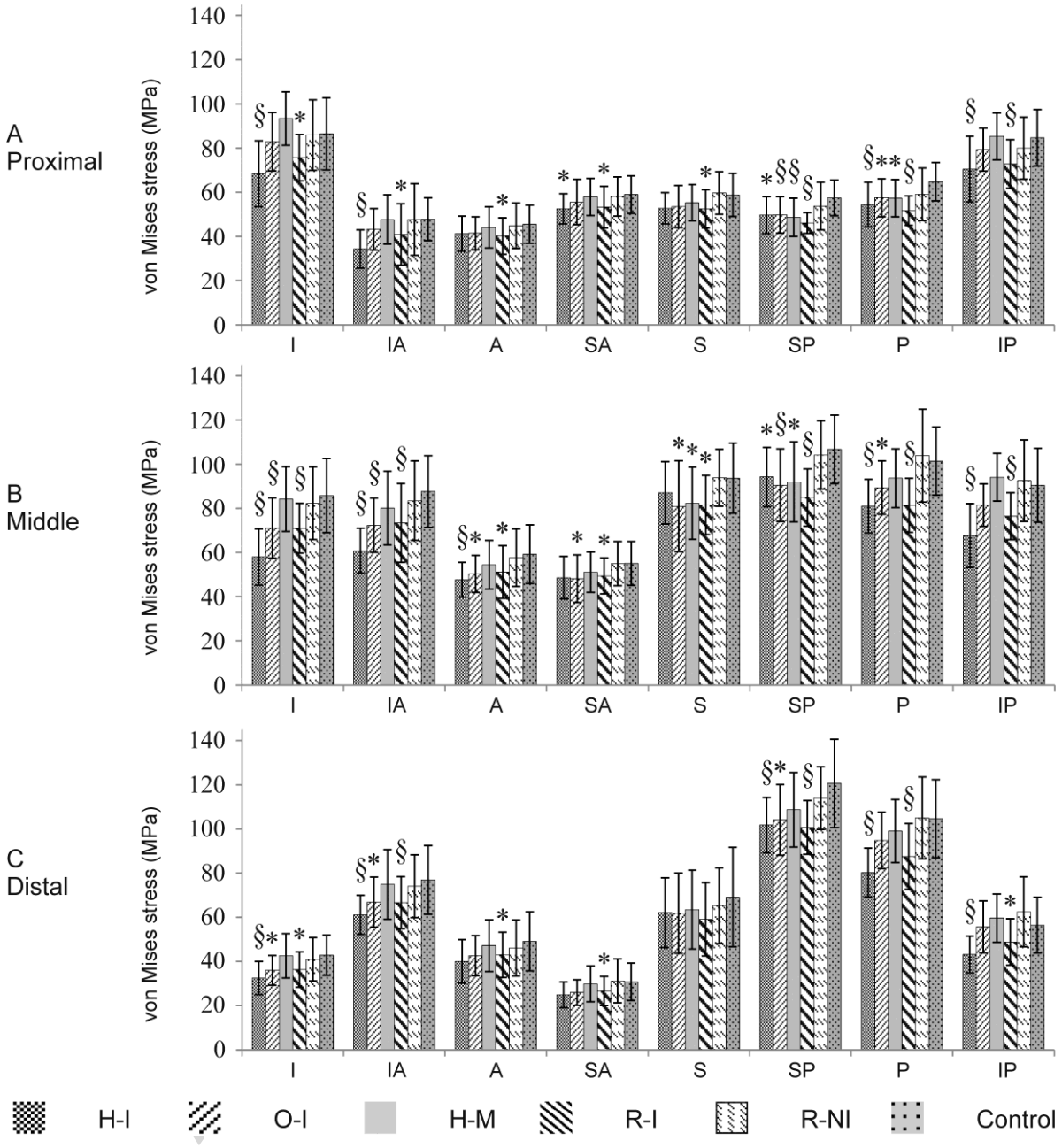

Figure 3

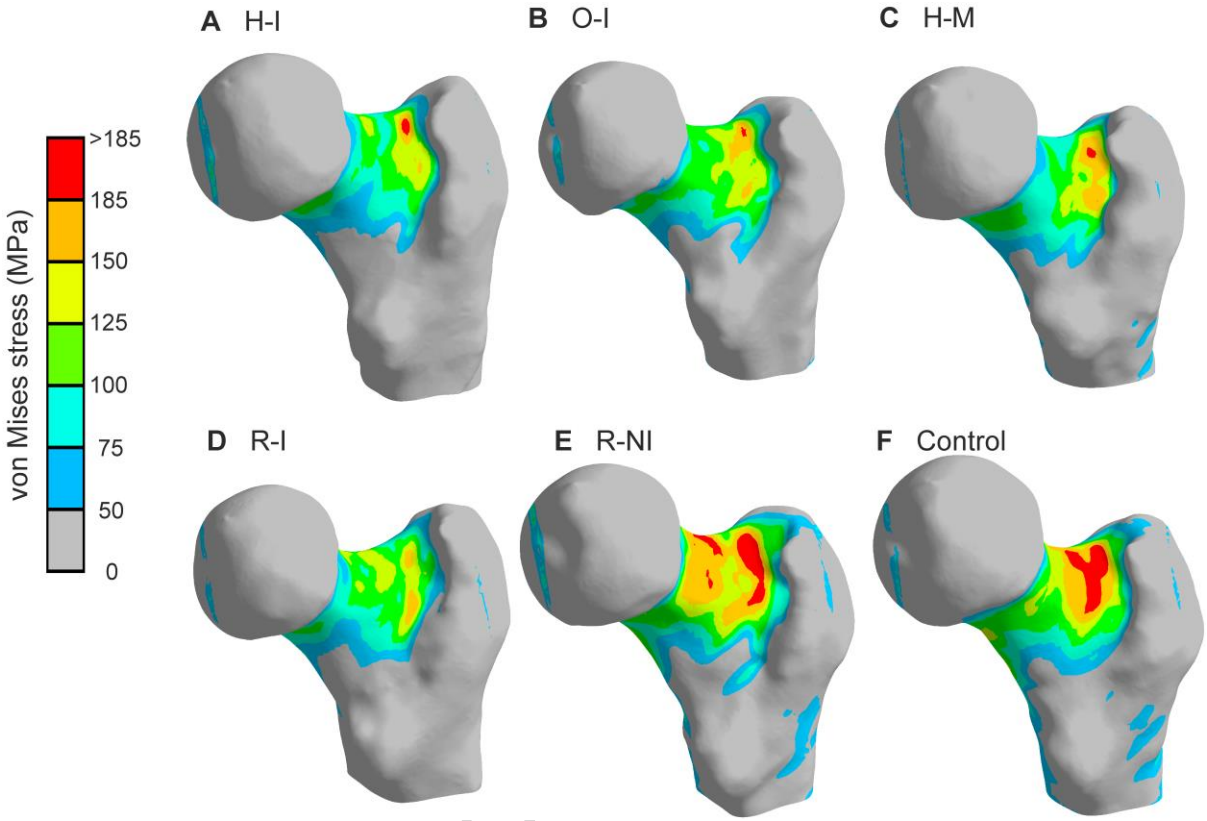

Figure 4

Highlights

- 3D FE analysis of proximal femur shows that loading history involving various impacts is associated with reduced fall-induced stress.
- The natural form of locomotion endurance running is equally efficient in terms of hip strength as extreme triple jumping.
- High vertical impacts, impacts from unusual directions, or repeated moderate impacts form a core set of exercises against hip fragility.